Journal of Molecular Graphics and Modelling 38 (2012) 354–359

Contents lists available at SciVerse ScienceDirect

Journal of Molecular Graphics and Modelling

journal homepage: www.elsevier.com/locate/JMGM

A DFT study on the interaction between adsorbed silver on C_{60} and disulfide bond

Khaled Azizi*, Ali Sohrabinia

Department of Chemistry, University of Kurdistan, Sanandaj, Iran

ARTICLE INFO

Article history:
Accepted 13 June 2012
Available online 26 June 2012

Keywords:
C_{60} fullerene
Silver atom
Disulfide bond
DMDS
HIV-1/gp 120

ABSTRACT

Adsorption of a silver atom on the surface of Buckyball (C_{60}) was investigated using density functional theory (DFT). The Ag atom tends to occupy the bridge site over C—C bond in pentagon–hexagon ring junction with the binding energy of −38.33 kcal mol^{-1}. The capability of destroying S—S bond by both a single silver atom and the silver atom adsorbed on C_{60} was also investigated by DFT calculations using dimethyl disulfide as the molecular model. The results of the natural bond orbital (NBO) and population analysis indicate that the cleavage of the S—S bond effectively occurs by the silver atom adsorbed on C_{60}. Since denaturation of disulfide bonds of envelope glycoprotein (gp) 120 is a key step in the prevention of the spread of HIV-1, the development of the proposed study is promised to HIV-1 research field.

1. Introduction

The discovery of the "buckyball" [1], has led to enormous interest in studying the properties of this kind of novel carbon structures. Metallofullerenes which form an important class of C_{60} derivatives have attracted much attention due to their unique physical and chemical properties and potential technological applications such as optical, electronic and magnetic materials, as well as radiotracers and magnetic resonance imaging contrast agents in medical sciences [2,3]. Exohedral metallofullerenes, in which a metal atom is bound outside the cage of C_{60}, are novel forms of fullerene-base materials which have been proposed as a promising candidate for both hydrogen storage [4] and applications in catalysis in carbon nano test tubes [5]. For instance, it has been identified that $Li_{12}C_{60}$ can bind 60 H_2 molecules (9 wt%) [6] and Na_8C_{60} can adsorb 48 H_2 molecules (9.5 wt%) [7]. Although the medical applications of fullerenes have been established [8], to the authors' knowledge no experimental or theoretical investigations have been devoted to the development of the medicinal applications of exohedral metallofullerenes, especially in drug transformation scope. Even though the adsorption of many transition metal atoms on C_{60} has already been studied [9], it has not been done for silver atoms. Our motivation for choosing Ag and studying the properties of AgC_{60} metallofulleren, comes from the Ag potential in medical applications.

The antibacterial activities of silver and silver-based compounds have been known for centuries [10]. In recent years, silver nanoparticles have also been intensively studied for their antimicrobial potential activity [11]. It has been proven that silver nanoparticles can act as an antiviral agent against the HIV-1 [12,13], hepatitis B virus [14], respiratory syncytial virus [15], herpes simplex virus type 1 [16] and monkeypox virus [17]. In fact, silver nanoparticles interact with outer membrane of bacteria and cause structural changes leading to degradation and finally to the death of the microbe [18]. For example, silver nanoparticles sized 1–10 nm can be attached to HIV-1 and prevent the virus from bonding to the host cells [19]. The HIV-1 envelope glycoprotein (gp) 120 is a highly disulfide-bonded molecule that attaches HIV-1 to the lymphocyte surface receptors, CD4 and CXCR4. The main factor associated with HIV-1 infection is the interaction between gp120 and CD4 [20]. The inhibitory activity of silver nanoparticles against the gp120–CD4 interaction has been confirmed [21]. The mechanism of the antiviral action of silver nanoparticles is closely related to their interaction with two disulfide bonds placed in the carboxyl half of the gp120, where the HIV-1 is bound to CD4 receptor [22,23]. It is suggested that silver nanoparticles should bind to gp120 knobs and change its properties by denaturing its disulfide-bonded domain placed in the CD4 binding region [24]. Therefore, the infection process is inhibited by the irreversible change of viral structure [21]. To denaturalize disulfide bond, one can consider a single Ag atom coming from silver nanoparticles and interacting with the disulfide bond. To the best of our knowledge the mechanism details of the interaction between silver nanoparticles and disulfide bond of the gp120 has not been reported so far.

In order to study the above-mentioned process, we took advantage of DFT method to investigate the possibility of the adsorption of silver atom on the outer surface of C_{60}. After obtaining this result that it is possible to intercalate an Ag atom on C_{60}, we tried to apply the AgC_{60} to cleave the S—S bond of DMDS. Furthermore, the methods used in our calculations are introduced and explained in detail.

* Corresponding author. Tel.: +98 871 6624133; fax: +98 871 6660075.
E-mail address: k.azizi@uok.ac.ir (K. Azizi).

1093-3263/$ – see front matter © 2012 Elsevier Inc. All rights reserved.
http://dx.doi.org/10.1016/j.jmgm.2012.06.003

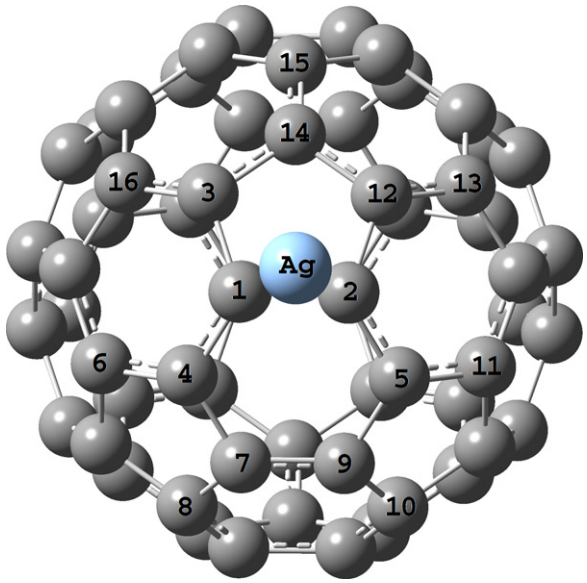

Fig. 1. The optimized structure of fullerene C_{60} with Ag atom adsorbed on the C—C bond in pentagon–hexagon ring junction. The labeled atoms are treated by 6-311G(d, p) basis set.

Finally, the possibility of cleavage of the S—S bond of DMDS by both single Ag atom and the Ag–C_{60} is also investigated.

2. Computational methods

All of the geometry optimization calculations were carried out using the DFT method within hybrid functional B3LYP (Becke's three-parameter [25] exchange functional employing the Lee, Yang, and Parr correlation functional) [26]. For all systems, an initial geometry optimization calculation was performed using 3-21G(d) basis set and the nature of optimized geometries for local minima was checked with frequency calculations. Further geometry optimizations were carried out as follows: Silver atom was treated by LanL2DZ basis set which uses a pseudo-potential function for the non-valence electrons and is widely used in study of compounds and clusters containing heavy elements [27,28]. In DMDS and Ag–DMDS, 6-311++G(d,p) basis set was used for carbon and hydrogen atoms and the sulfur atoms were treated by aug-cc-pVQZ basis set which can give rise to reasonable results for molecules including sulfur atoms [29]. In the adsorption process of one Ag atom by C_{60}, we considered three initial configuration; Ag at the center of a hexagon ring, Ag at the center of a pentagon ring and Ag located on a single carbon atom. In the first case, the carbon atoms forming the hexagon ring (carbons with labels 1, 2, 4, 5, 7 and 9 as shown in Fig. 1) and also those carbon atoms attached to them (atoms specified by labels 3, 6, 8, 10, 11 and 12) were treated by 6-311G(d,p) basis set. We did exactly the same procedure for the second case, i.e. Ag at the center of a pentagon ring. In the third case, carbon atom 2 (see Fig. 1) on which Ag atom located and its nearest neighbors (atoms labeled by 1, 5 and 12) were treated by 6-311G(d,p) basis set. The rest of the carbon atoms which were not mentioned above are treated with the commonly used 3-21G(d) basis set. All the structural parameters were fully optimized without any symmetry constraints. In all cases, in order to confirm that the optimized geometries correspond to a real minimum at the potential energy surface and also to quantify the zero-point vibrational energy correction, vibrational frequency calculations were performed at the same level of theory.

Single-point energy and NBO calculations were carried out using the exchange–correlation functional of Perdew and Wang (PW91) [30] which has been demonstrated that provides a more accurate dispersion force than B3LYP [31,32]. Silver and sulfur atoms were treated with LanL2DZ and aug-cc-pVQZ basis sets, respectively and all the carbon and hydrogen atoms were treated by 6-311++G(d,p) basis set. The binding energy, E_{ad}, was obtained as the difference between the energy of the complex (AB) and the combination of the energies of the isolated species A and B [33,34],

$$E_{ad} = E_{AB} - (E_A + E_B) \quad (1)$$

Local charge and orbital occupancies at each atom were calculated according to natural bond orbital (NBO) and population analysis. All calculations on the isolated species and molecular complexes were performed using the GAUSSIAN 98 program package [35].

Table 1
Bond lengths and NPA charge of silver atom and its six nearest neighbor carbon atoms in C_{60} and AgC_{60}.

Atom–atom distance	Bond length (Å)		Atom number	NPA charge $\|e\|$
	C_{60}	AgC_{60}		
Ag—C(1)	–	2.388	Ag	0.599
Ag—C(2)	–	2.423	C(1)	−0.147
C(1)–C(2)	1.448	1.470	C(2)	−0.152
C(1)–C(3)	1.448	1.455	C(3)	−0.056
C(1)–(C4)	1.388	1.402	C(4)	−0.031
C(2)–C(5)	1.388	1.399	C(5)	−0.027
C(2)–(C12)	1.448	1.454	C(12)	−0.043

Table 2
The energies of the HOMO, the LUMO and the difference between the energies of frontier orbitals, $\Delta E_{F.O}$ for C_{60} and Ag atom.

	E_{HOMO} (eV)	E_{LUMO} (eV)	$\Delta E_{F.O}$[a] (eV)
C_{60}	−0.237	−0.137	0.218[b]
Ag	−0.192	−0.019	0.055[c]

[a] Frontier orbital.
[b] $\left|E_{HOMO(C_{60})} - E_{LUMO(Ag)}\right|$.
[c] $\left|E_{HOMO(Ag)} - E_{LUMO(C_{60})}\right|$.

3. Results and discussion

3.1. Adsorption of silver atom on C_{60} surface

We examined the adsorption site on which an Ag atom can give rise to the highest adsorption energy on the C_{60} surface. Three different initial sites were tested, including the top site of the carbon atom, the hollow site of the hexagon ring and the hollow site of the pentagon ring. After full structural optimization, the Ag atom was always located on the C—C bond in pentagon–hexagon ring junction, regardless of its initial location. Fig. 1 shows the optimized geometry of Ag atom on C_{60} surface in gas phase. The electronic and structural properties of AgC_{60} including atom–atom distance and natural population analysis (NPA) charge of Ag atom along with its six nearest carbon atoms are summarized in Table 1. It can be seen that the length of C—C bond on which the Ag atom sits, C(1)–C(2), and its adjacent bonds are increased due to the adsorption of Ag on C_{60} surface. These bond-length changes may be attributed to the significant electron transfer from the highest occupied molecular orbital (HOMO) of Ag to the lowest unoccupied molecular orbital (LUMO), π^*, of carbon atom in C_{60}.

The energies of the HOMO and LUMO of Ag, C_{60} and AgC_{60} are listed in Table 2. The results show that the energy difference $\left|Ag_{(HOMO)} - C_{60(LUMO)}\right|$ is considerably smaller than $\left|C_{60(HOMO)} - Ag_{(LUMO)}\right|$. Therefore, based on the theory of frontier molecular orbitals, a significant overlap and electron density transfer can be performed between the HOMO of Ag and the LUMO of

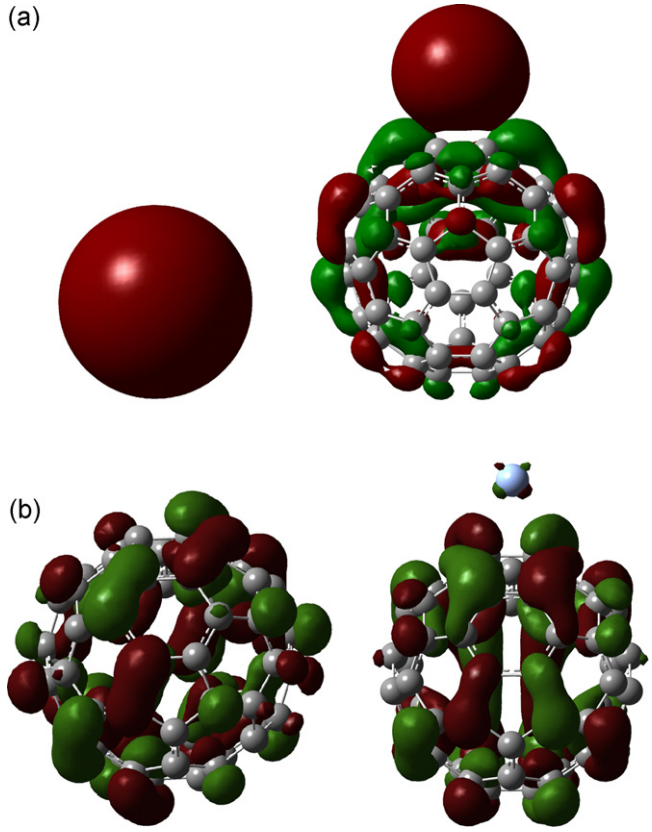

Fig. 2. The electronic density similarity (a) between the high occupied molecular orbital (HOMO) of Ag and AgC_{60} and (b) between the lowest unoccupied molecular orbital (LUMO) of C_{60} and AgC_{60}.

C_{60}, which result in a considerable amount of adsorption energy [36–38].

Fig. 2 shows schematic diagrams of the HOMO of Ag, the LUMO of C_{60} and the HOMO and LUMO of AgC_{60}. It can be seen that charge distributions in $(AgC_{60})_{HOMO}$ and $Ag_{(HOMO)}$ are similar to each other and there is a similarity between $(AgC_{60})_{LUMO}$ and $(C_{60})_{LUMO}$ as well. Therefore, it is reasonable to expect that in electrophilic reactions including AgC_{60}, $Ag_{(HOMO)}$ plays a major role.

The charge transfer from Ag to the C_{60} cage makes the Ag atom interact electrostatically with the C_{60}. In fact, the results of NPA indicate that the Ag carries a charge of $0.6|e|$, and as the data in Table 1 shows, about 75% of the charge is transferred to the Ag six nearest-neighbor carbon atoms. It suggests that the interaction between Ag and C_{60} has significant ionic character which leads to an adsorption energy equal to -38.33 kcal mol^{-1}.

Unfortunately, experimental results are not available for evaluation of our predictions. However, our results may be compared with those obtained for adsorption of lithium atom on the surface of C_{60} [6]. The charge transfers from Li to C_{60}, and adsorption energy of single Li atom on the surface of C_{60} were given as $0.75|e|$ and 41.3 kcal mol^{-1}, respectively. Considering the first ionization energies of Li (125 kcal mol^{-1}) and Ag (176 kcal mol^{-1}) [39], the smaller charge transfer to C_{60} from Ag in comparison with Li is plausible. On the other hand, stronger electrostatic interactions and larger amount of binding energy are expected for Li due to its larger amount of electrostatic charge. However, it should be noted that difference of the binding energy values of Li and Ag atoms to the surface of C_{60} is too small to be only due to the electrical charge difference. It seems that the role of the dispersion forces in binding energies should also be considered which is expected to be more important for Ag than Li, due to the large number of valence electrons of Ag compared to that of Li.

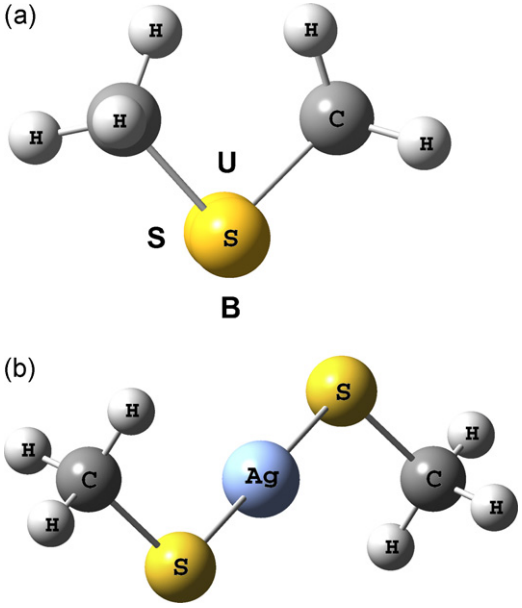

Fig. 3. (a) Three initial geometries, up (U), one side (S) and below (B) considered for interaction between an Ag atom and DMDS, (b) the optimized structure of Ag–DMDS.

3.2. The interaction between silver atom and disulfide bond

The interaction between AgC_{60} and DMDS may be considered as a combination of two steps, an initial step of separation of Ag from C_{60}, followed by a second step of interaction between Ag and DMDS. On the other hand, the interaction between an Ag atom separated from silver nanoparticles and disulfide bond of HIV-1 envelope glycoprotein (gp) 120 may be considered as one of the possible processes. Therefore, it is reasonable to study how an Ag atom interacts with disulfide bond of DMDS. As can be seen in Fig. 3, three initial locations are considered for interaction between Ag and DMDS. The initial locations of Ag atom with respect to the disulfide bond are specified as "B", the geometry in which Ag atom locates near the disulfide bond and far from methyl groups, "U", in which Ag atom locates between two methyl groups, and "S", in which Ag atom locates on the one side of the DMDS molecule.

The results of geometry optimization indicate that among three initial locations only "B" geometry leads to interaction between Ag atom and disulfide bond of DMDS. The results of natural bond orbital (NBO) analysis confirm the cleavage of disulfide bond of DMDS and formation of two Ag—S bonds, as shown in Fig. 3(b). The S—Ag—S angle is 180° and the relative orientation of S-methyl groups turns from *cis* conformer in DMDS to *trans* conformer in Ag–DMDS.

Using formula 1, the energy of interaction between Ag and DMDS is calculated to be -75.36 kcal mol^{-1}. The zero point energy correction is negligible and cannot seriously affect the amount of binding energy. The change in the values of internal energy, ΔE, enthalpy, ΔH, and Gibbs free energy, ΔG, of the reaction at room temperature are calculated to be -69.88 kcal mol^{-1}, -68.1 kcal mol^{-1} and -68.92 kcal mol^{-1}, respectively. A comparison between the absolute values of molar sublimation energy of silver, 56.76 kcal mol^{-1} [39] and binding energy of Ag to DMDS either at 0 K (75.36 kcal mol^{-1}) or at 298 K (-68.1 kcal mol^{-1}) indicates that the proposed process for interaction between silver nanoparticles and highly disulfide-bonded HIV-1 envelope glycoprotein (gp) 120 is energetically favorable. Further discussions on

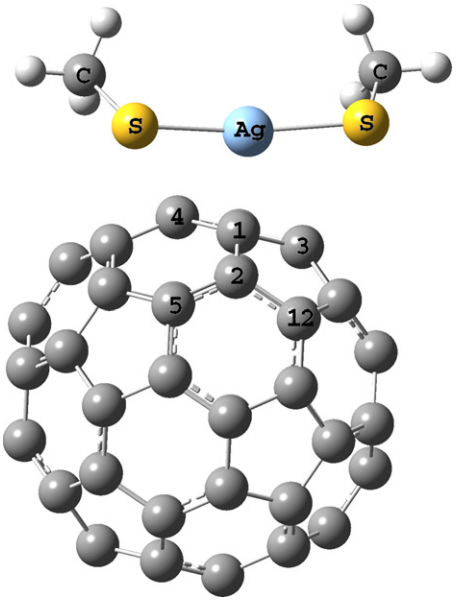

Fig. 4. The optimized structure of AgC_{60}–DMDS and effective cleavage of disulfide bond of DMDS by an Ag atom adsorbed on C_{60}.

the structural and electronic parameters of Ag–DMDS are postponed for the next section.

3.3. The interaction between AgC_{60} and disulfide bond

In order to investigate the capability of AgC_{60} in destroying the disulfide bond, which plays a key role in attaching HIV-1/gp120 to the lymphocyte surface receptors, CD4, [20], the interaction between AgC_{60} and DMDS, as a simple example, was studied by the DFT method. As in the case of interaction between Ag and DMDS, three initial configurations, B, U and S were chosen for interaction between AgC_{60} and DMDS. Again, only "B" geometry leads to disulfide bond cleavage and Ag—S bonds formation, as can be seen in Fig. 4. A comparison between desorption energy of atomic Ag on C_{60} surface, 38.33 kcal mol^{-1}, and molar sublimation energy of silver, 56.76 kcal mol^{-1} [40] indicates that energetically it is more favorable for disulfide bond to be added to AgC_{60} than to Ag nanoparticles, assuming that in both cases the initial reaction which leads to the cleavage of disulfide bond is made by a single Ag atom. Furthermore, the HOMO–LUMO energy gap of AgC_{60} (24.6 kcal mol^{-1}) is significantly smaller than that of both C_{60} (67.176 kcal mol^{-1}) and Ag (92.8 kcal mol^{-1}), which in turn strengthens the reaction between AgC_{60} and disulfide bond. In addition, the interaction between AgC_{60} and disulfide bond is facilitated by partial positive and negative charges centered on Ag and S atoms, respectively.

A comparison between Figs. 3 and 4 show that in both Ag–DMDS and AgC_{60}–DMDS structures, the disulfide bond is broken into two separated S-methyl units, although the geometries of S-methyl units with respect to S—S bond are not similar to each other. It should be noted that in AgC_{60}–DMDS structure, there is a weak interaction between Ag and C_{60} and they are not completely separated from each other. The main reason is that in AgC_{60}–DMDS structure the total charge of C_{60} is $-0.07|e|$ and the occupancy of valance orbitals of the nearest-neighbor carbon atoms to Ag, (C(1),C(2)) is calculated to be 2s(0.87)2p(3.15) which is slightly different from that of carbon atoms in pristine C_{60}, 2s(0.86)2p(3.13). Therefore, in AgC_{60}–DMDS structure, the rotation of S-methyl groups around S—Ag bonds is limited due to the presence of C_{60}. Three dimensional pictures of HOMO and LUMO which are shown

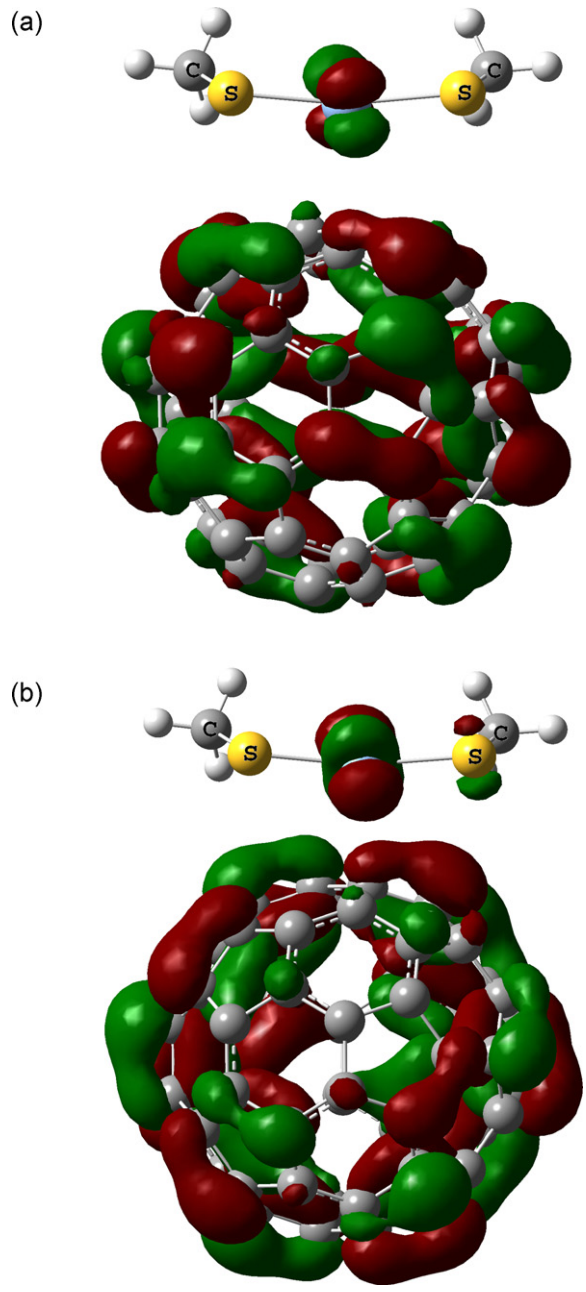

Fig. 5. The electronic densities for (a) HOMO and (b) LUMO of AgC_{60}–DMDS, represent the existence of weak dispersion forces between Ag atom and C_{60}.

in Fig. 5, also confirm the existence of surrounding electronic density and hence the existence of dispersion forces between Ag and C_{60} in AgC_{60}–DMDS structure.

Furthermore, the distance between Ag atom and the nearest carbon atom in AgC_{60}, C(1), increases from 2.39 Å to 2.84 Å in AgC_{60}–DMDS, which is out of the range of chemical bonding length and should be considered as a physisorption distance. Therefore, Ag prefers DMDS to C_{60}. This can be considered as an important reason for separating Ag from C_{60} and its interaction with DMDS. The results of NBO calculations also confirm the cleavage of S—S bond and the formation of the two Ag—S bonds in both Ag–DMDS and AgC_{60}–DMDS structures. These results are in agreement with increasing of the S—S distance from 2.115 Å in DMDS to 4.573 Å and 4.567 Å in Ag–DMDS and AgC_{60}–DMDS structures, respectively.

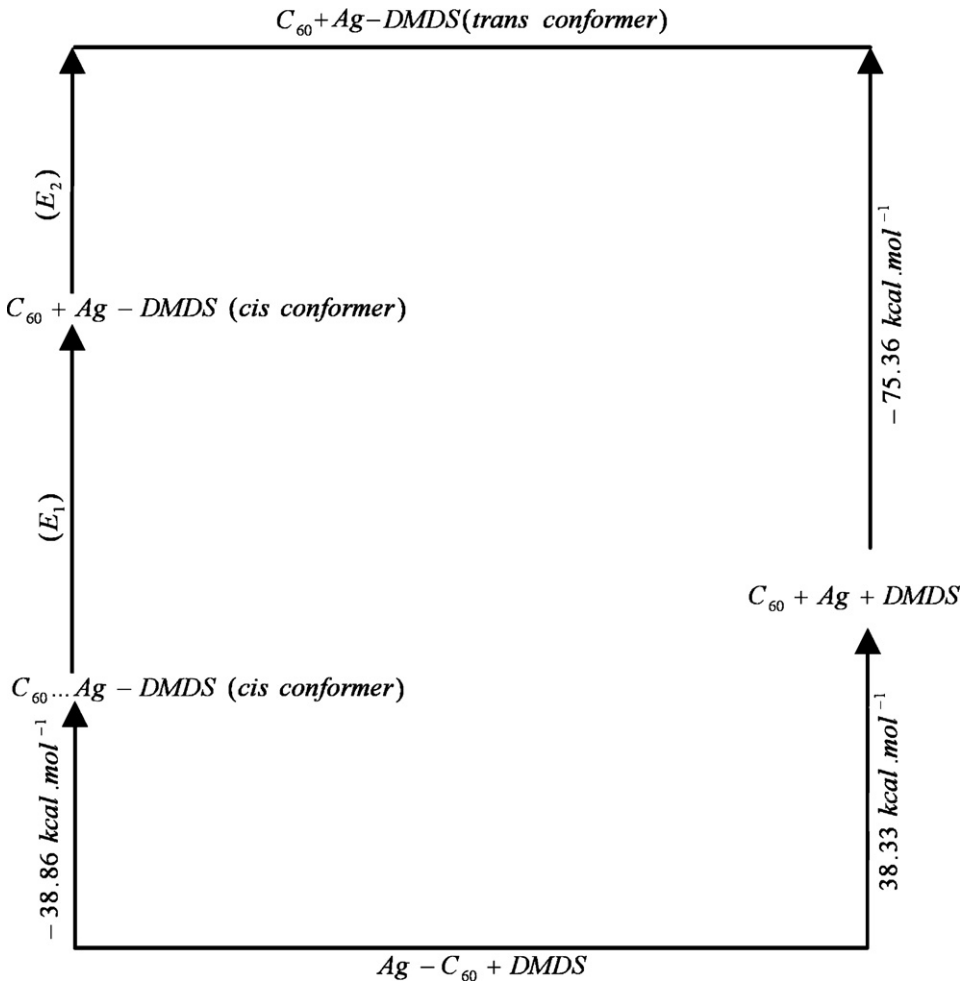

Fig. 6. Energy change diagram for the reaction between Ag–C_{60} and DMDS.

The energy of interaction between AgC_{60} and DMDS is calculated to be −36.86 kcal mol^{-1}. In Fig. 4, let us suppose, for a moment, that the Ag atom and C_{60} are completely isolated from each other and the S—Me groups are in *trans* conformation. Therefore, the energy of reaction is the sum of the energy required for desorption of the Ag from C_{60} (38.33 kcal mol^{-1}) and the energy of interaction between the Ag atom and DMDS (−75.36 kcal mol^{-1}), which is −37.03 kcal mol^{-1}. Fig. 6 indicates the different steps of the interaction between Ag—C_{60} and DMDS in detail. As can be seen in Fig. 6, the error caused by the above-mentioned assumptions is negligible. In order to estimate the amount of the energy corresponding to each of the two assumptions, we set up a single point calculation on the structure of Ag–DMDS (Fig. 4, without C_{60}) at the same level of the computation mentioned in section II. The analysis of the results of this calculation indicates that the *trans* conformer of Ag–DMDS about 2.0 kcal mol^{-1} is more stable than *cis* conformer. Therefore, according to Fig. 6 the energy of binding of C_{60} to Ag–DMDS is estimated to be 3.83 kcal mol^{-1} and we can conclude that the Ag atom is effectively isolated from the C_{60} and interacts with DMDS.

It has been shown that the basis set superposition error (BSSE) correction for a DFT/LanL2DZ calculation including the interaction between Ag atom and C=C bond including molecules as alkenes is about 0.8 kcal mol^{-1} [41]. Therefore, we expect that the BSSE correction for interaction between Ag atom and C_{60} should be about the same amount of the energy and does not affect our results. It seems that the reason of small BSSE correction is related to the large amount of charge transfer from Ag atom to C_{60} or the molecule containing C=C bond. In this case the nature of the interaction between Ag atom and C_{60} molecule is more electrostatic than van der Waals. Therefore, the BSSE correction which is related to dispersion forces can be ignored in our calculations.

The results of this research show that C_{60} can be used as a good carrier for Ag atom and the adsorbed Ag on C_{60} has capability of interacting and cleaving the disulfide bond in DMDS. Assuming that the proposed process is true, the AgC_{60}, as a disulfide bond destroyer, can be a good candidate for further studies on its capability in destroying the disulfide bond of gp120 and preventing the junction between HIV-1 and CD4.

4. Conclusion

DFT calculations confirm the physisorption of an Ag atom on the outer surface of C_{60} fullerene. In AgC_{60} structure, the adsorbed Ag atom is located on the bridge site over C—C bond in pentagon–hexagon ring junction. The adsorption energy of Ag atom on the surface of C_{60} was calculated to be −38.33 kcal mol^{-1} which is in agreement with the results that were obtained for adsorption of Li on the surface of C_{60} [6]. Based on the results of NPA calculations the Ag carries a charge of 0.6|*e*|, suggesting that the adsorption energy of Ag on C_{60} surface is essentially due to electrostatic interactions. Destroying the disulfide bond of DMDS by both a single Ag atom and an Ag atom adsorbed on the outer surface of C_{60} was confirmed by the results of DFT and NBO calculations. It is expected that

AgC_{60} can show the same capability in interaction with the disulfide bond of HIV-1/gp120 and can result in decreasing the activity of HIV-1 by causing a perturbation in gp120–CD4 receptor interaction.

References

[1] H.W. Kroto, J.R. Heath, S.C. O'Brien, R.F. Curl, R.E. Smalley, C_{60}: Buckminsterfullerene, Nature 318 (1985) 162–163.
[2] L.J. Wilson, Medical applications of fullerenes and metallofullerenes, Electrochemical Society Interface 8 (4) (1999) 24–28.
[3] T. Da Ros, M. Prato, Medicinal chemistry with fullerenes and fullerene derivatives, Chemical Communications (1999) 663–669.
[4] M. Yoon, S. Yang, Z. Zhang, Interaction between hydrogen molecules and metallofullerenes, Journal of Chemical Physics 131 (6) (2009), 64707-1–64707-5.
[5] T.W. Chamberlain, N.R. Champness, M. Schröder, A.N. Khlobystov, A Piggyback ride for transition metals; encapsulation of exohedral metallofullerenes in carbon nanotubes, Chemistry: A European Journal 17 (2011) 668–674.
[6] Q. Sun, P. Jena, Q. Wang, M. Marquez, First-principles study of hydrogen storage on $Li_{12}C_{60}$, Journal of the American Chemical Society 128 (2005) 9741–9745.
[7] K.R.S. Chandrakumar, S. Ghosh, Alkali-metal-induced enhancement of hydrogen adsorption in C-60 fullerene: an ab initio study, Nano Letters 8 (2008) 13–19.
[8] R. Bakry, R.M. Vallant, M. Najam-ul-Haq, M. Rainer, Z. Szabo, C.W. Huck, G.K. Bonnv, Medicinal applications of fullerenes, International Journal of Nanomedicine 2 (4) (2007) 639–649.
[9] O. Loboda, A DFT study on exohedral metallofullerenes: structural and electronic properties, Fullerenes, Nanotubes and Carbon Nanostructures 17 (2009) 457–475.
[10] S.Y. Liau, D.C. Read, W.J. Pugh, J.R. Furr, A.D. Russell, Interaction of silver nitrate with readily identifiable groups: relationship to the antibacterial action of silver ions, Letters in Applied Microbiology 25 (1997) 279–283.
[11] J.S. Kim, E. Kuk, K.N. Yu, J.H. Kim, S.J. Park, H.J. Lee, S.H. Kim, Y.K. Park, Y.H. Park, C.Y. Hwang, Y.K. Kim, Y.S. Lee, D.H. Jeong, M.H. Cho, Antimicrobial effects of silver nanoparticles, Nanomedicine 3 (2007) 95–101.
[12] R.W. Sun, C. Rong, N.P. Chung, C.M. Ho, C.L. Lin, C.M. Che, Silver nanoparticles fabricated in Hepes buffer exhibit cytoprotective activities toward HIV-1 infected cells, Chemical Communications (2005) 5059–5061.
[13] M.A. Mastro, W.A. Hardy, A. Boasso, G.M. Shearer, C.R. Eddy, F.J. Kub, Non-toxic inhibition of HIV-1 replication with silver–copper nanoparticles, Medicinal Chemistry Research 19 (2009) 1074–1081.
[14] L. Lu, R.W. Sun, R. Chen, C.K. Hui, C.M. Ho, J.M. Luk, G.K. Lau, C.M. Che, Silver nanoparticles inhibit hepatitis B virus replication, Antiviral Therapy 13 (2008) 253–262.
[15] L. Sun, A.K. Singh, K. Vig, S.R. Pillai, S.R. Singh, Silver nanoparticles inhibit replication of respiratory syncytial virus, Journal of Biomedicine and Biotechnology 4 (2008) 149–158.
[16] D. Baram-Pinto, S. Shukla, N. Perkas, A. Gedanken, R. Sarid, Inhibition of herpes simplex virus type 1 infection by silver nanoparticles capped with mercaptoethane sulfonate, Bioconjugate Chemistry 20 (2009) 1497–1502.
[17] J.V. Rogers, C.V. Parkinson, Y.W. Choi, J.L. Speshock, S.M. Hussain, A preliminary assessment of silver nanoparticle inhibition of monkeypox virus plaque formation, Nanoscale Research Letters 3 (2008) 129–133.
[18] A. Kumar, P.K. Vemula, P.M. Ajayan, G. John, Silver-nanoparticle-embedded antimicrobial paints based on vegetable oil, Nature Materials 10 (2008) 236–241.
[19] J.L. Elechiguerra, J. Burt, J.R. Morones, B.A. Camacho, X. Gao, H.H. Lara, Y. Jose, Interaction of silver nanoparticles with HIV-1, Journal of Nanobiotechnology 3 (6) (2005) 1477–3155.
[20] R. Barbouche, R. Miquelis, I.M. Jones, E. Fenouillet, Protein-disulfide isomerase-mediated reduction of two disulfide bonds of HIV envelope glycoprotein 120 occurs post-CXCR4 binding and is required for fusion, Journal of Biological Chemistry 278 (2003) 3131–3136.
[21] H.H. Lara, V.N. Ayala-Nunez, L. Ixtepa -Turrent, L.C. Rodriguez-Padilla, Mode of antiviral action of silver nanoparticles against HIV-1, Journal of Nanobiotechnology 8 (2010) 1–10.
[22] C. Lekutis, U. Olshevsky, C. Furman, M. Thali, J. Sodroski, Contribution of disulfide bonds in the carboxyl terminus of the human immunodeficiency virus type1 gp120 glycoprotein to CD4 binding, Journal of Acquired Immune Deficiency Syndrome 5 (1992) 78–81.
[23] J.P. Sinclair, W.T. Shearer, Current status of CD4-based therapies for prophylaxis and treatment of HIV infection, Biodrugs 8 (1997) 128–138.
[24] G.E. McDonnell, Antisepsis, Disinfection, and Sterilization: Types, Action and Resistance, ASM press, Washington, DC, 2007.
[25] A.D. Becke, Density-functional thermochemistry. III. The role of exact exchange, Journal of Chemical Physics 98 (1993) 5648–5652.
[26] C. Lee, W. Yang, R.G. Parr, Development of the Colle–Salvetti correlation-energy formula into a functional of the electron density, Physical Review 37 (1988) 785–789.
[27] P.J. Hay, W.R. Wadt, *Ab initio* effective core potentials for molecular calculations. Potentials for the transition metal atoms Sc to Hg, Journal of Chemical Physics 82 (1985) 270–283.
[28] J.G. Han, F. Hagelberg, A density functional theory investigation on CrSin (n = 1–6) clusters, Chemical Physics 263 (2001) 255–262.
[29] P.A. Denis, Basis set requirements for sulfur compounds in density functional theory: a comparison between correlation-consistent, polarized-consistent, and Pople-type basis sets, Journal of Chemical Theory and Computers 1 (2005) 900–907.
[30] J.P. Perdew, Y. Wang, Accurate and simple analytic representation of the electron–gas correlation energy, Physical Review B 45 (1992) 13244–13249.
[31] W.B. De Almeida, An investigation of the dispersion forces in weakly bound complexes using quantum chemical and multipole expansion, Journal of the Brazilian Chemical Society 16 (3A) (2005) 345–361.
[32] J. Lan, D. Cheng, D. Cao, W. Wang, Silicon nanotube as a promising candidate for hydrogen storage from the first principle calculations to grand canonical Monte Carlo simulations, Journal of Physical Chemistry C 112 (2008) 5598–5604.
[33] P. Hobza, R. Zahradnik, Intermolecular complexes, Elsevier, Amsterdam, 1988.
[34] F.B. van Duijneveldt, J.G.C.M. van Duijneveldt-van de Rijdt, J.H. van Lenthe, State of the art in counterpoise theory, Chemical Reviews 94 (1994) 1873–1885.
[35] M.J. Frisch, G.W. Trucks, H.B. Schlegel, G.E. Scuseria, M.A. Robb, J.R. Cheeseman, V.G. Zakrzewski, J.A. Montgomery Jr., R.E. Stratmann, J.C. Burant, S. Dapprich, J.M. Millam, A.D. Daniels, K.N. Kudin, M.C. Strain, Ö. Farkas, J. Tomasi, V. Barone, M. Cossi, R. Cammi, B. Mennucci, C. Pomelli, C. Adamo, S. Clifford, J. Ochterski, G.A. Petersson, P.Y. Ayala, Q. Cui, K. Morokuma, P. Salvador, J.J. Dannenberg, D.K. Malick, A.D. Rabuck, K. Raghavachari, J.B. Foresman, J. Cioslowski, J.V. Ortiz, A.G. Baboul, B.B. Stefanov, G. Liu, A. Liashenko, P. Piskorz, I. Komáromi, R. Gomperts, R.L. Martin, D.J. Fox, T. Keith, M.A. Al-Laham, C.Y. Peng, A. Nanayakkara, M. Challacombe, P.M.W. Gill, B. Johnson, W. Chen, M.W. Wong, J.L. Andres, C. Gonzalez, M. Head-Gordon, E.S. Replogle, J.A. Pople, Gaussian 98, Gaussian, Inc., Pittsburgh, PA, 1998.
[36] L.S. Wang, S.K. Han, Structure, Properties and Activity of Molecules, Chemical Engineering Industry Press, Beijing, 1997.
[37] M. Ozcan, F. Karadag, I. Dehri, Interfacial behavior of cysteine between mild steel and sulfuric acid as corrosion inhibitor, Acta Physica Chimica Sinica 24 (2008) 1387–1392.
[38] W. Huang, Y. Tan, B. Chen, J. Dong, X. Wang, The binding of antiwear additives to iron surfaces: quantum chemical calculations and tribological tests, Tribology International 36 (2003) 163–168.
[39] D.R. Lide, CRC Handbook of Chemistry and Physics, vol. 84, CRC Press, 2003.
[40] K.K. Nanda, A. Maisels, F.E. Kruis, H. Fissan, S. Stappert, Higher surface energy of free nanoparticles, Physical Review Letters 91 (2003) 106102.
[41] J. Kaneti, L.C.P.M. de Smet, R. Boom, H. Zuilhof, E.J.R. Sudholter, Computational probes into the basis of silver ion chromatography. II. Silver(I)–olefin complexes, Journal of Physical Chemistry A 106 (2002) 11197–11204.